European Drag Reduction and Flow Control Meeting – EDRFCM 2015
March 23–26, 2015, Cambridge, UK

Control of the Leading-edge Flow Separation using DBD Plasma Actuators

Longfei Song and Kwing-So Choi
Faculty of Engineering, University of Nottingham, NG7 2RD, Nottingham, UK

INTRODUCTION

The dielectric-barrier-discharge (DBD) plasma actuators are some of the most promising active flow control techniques that could improve the aerodynamics of airfoil. They have a number of applications for flow control, including flow separation control of airfoils [1][2], pitching and roll moment control of aircraft [3][4], skin-friction reduction [5][6] and so on. In this study, our interest is on flow separation control at the leading edge of an airfoil. Previously, wall jets or vortex generators based on the DBD plasma actuator were used to control the flow separation. Here, a new concept of virtual drooped nose is being developed to achieve the separation control. PIV measurements were conducted to investigate the flow induced by plasma actuators, so that an understanding of how they affect the flow around the leading-edge of an airfoil could be obtained.

EXPERIMENTAL SETUP

A 3D printed NACA 0012 airfoil with a chord length of 100mm and a span of 250mm was made and used as a test model. It is supported by a rod at 25% of the chord length from the leading-edge, which was mounted to the test section of the wind tunnel.

The centreline of the DBD plasma actuator is placed at the leading-edge at $x/c = y/c = 0$. The actuator consists of two exposed electrodes and an embedded electrode, separated by a Kapton dielectric sheet. All the three electrodes have a width of 10mm, 0.035mm thick. The thickness of the Kapton dielectric sheet is 0.065mm. The actuator is driven by PSI-MCPG2503C power supply from KI Tech Ltd., which produces a sinusoidal voltage signal to the plasma actuator with a maximum power of 150W.

The experiment is conducted with a time-resolved PIV system, which consists of a Litron LDY 302 PIV 100W Nd: YLF laser, a SpeedSense 9060 high-speed camera and a computer. Olive oil is used to uniformly seed the air inside the chamber through the atomiser with 1- μm-diameter droplets from TSI 9307-6 oil droplet generator. The laser has a maximum output of 100 W at a bursting frequency of 10000 Hz and the wave length is 527 nm. The field of view is 80mm×50mm with resolutions of 1200×800 pixels in image width and height directions, respectively. Each image is exposed to 10 ns laser pulse.

Analysis is conducted to calculate the velocity field and vorticity field using Dynamic Studio 3.40. A recursive cross-correlation technique is used to compute the velocity vectors of the flow field around the plasma actuator. The velocity vectors were computed on small interrogation windows with 50% overlap in both horizontal and vertical directions. Filters were adopted to validate the velocity vectors by calculating the deviation from the surrounding vectors. This usually results in less than 5% erroneous vectors, which would be replaced by interpolation of the velocity vectors nearby.

RESULTS

PIV measurements of several different cases were conducted. To explain in details, here we just present the results of just one case with voltages of 6kV applied to the exposed electrode attached on the upper surface and 5.5kV to the exposed lower-surface electrode. The frequency of these sinusoidal voltages is 34 kHz.

The time-averaged velocity plus vorticity field is shown in

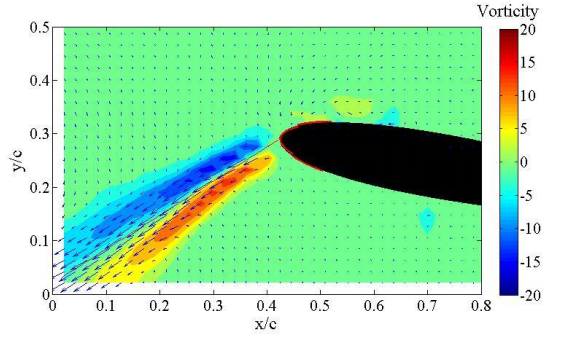

(a)

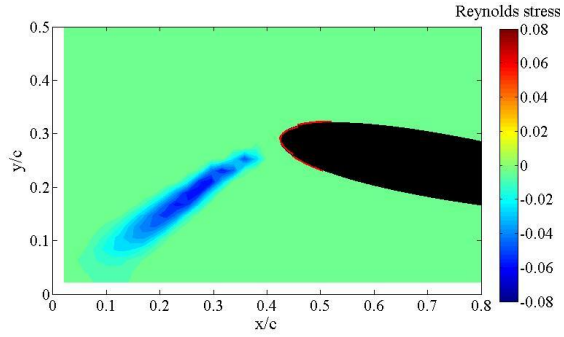

(b)

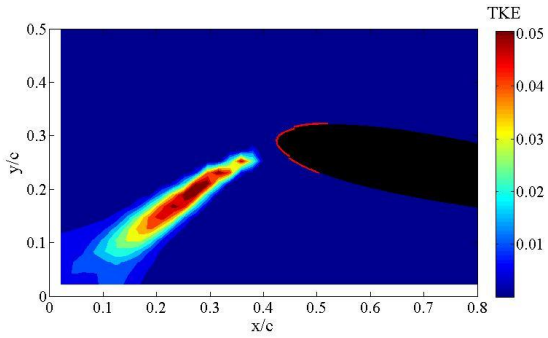

(c)

Figure 1 PIV measurement of the flow around a NACA 0012 airfoil with an angle of attack of 10 degrees: (a) time-averaged velocity field plus vorticity field; (b) Reynolds stress field; (c) turbulent kinetic energy distribution.

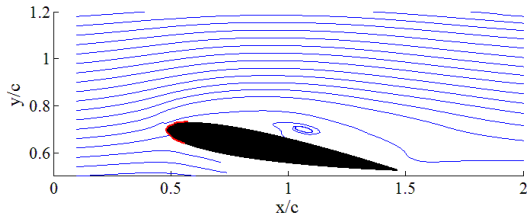

(a)

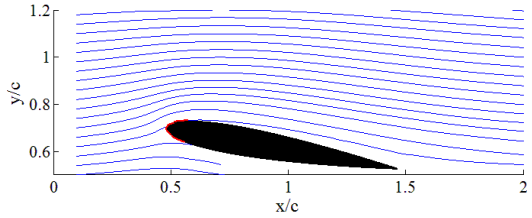

(b)

Figure 2 Streamlines of the time-averaged flow around a NACA 0012 airfoil at AOA=10° with freestream velocity of 3m/s: (a) without plasma; (b) with plasma

Figure 1 (a), from which we can see a plasma jet is generated around the leading-edge of the NACA 0012 airfoil. This jet goes opposite to the freestream and moves downwards with an angle of 44° to the chord of the airfoil.

The Reynolds stress field is calculated as well and shown in Figure 1 (b). Reynolds stress increases during the formation of the plasma jet, which means that turbulence develops in the plasma jet. Figure 1 (c) gives the distribution of the turbulent kinetic energy. The turbulent kinetic energy increases when the plasma jet develops, this shows that the plasma actuator entrains external energetic fluids from the external flows, therefore a virtual shape is formed around the leading-edge of the airfoil and this could probably act as a "virtual nose droop".

Error! Reference source not found. presents the streamlines of the time-averaged flow field around the airfoil when the freestream velocity is 3m/s and the angle of attack is set at 10° . It can be seen in Figure 2 (a) that the flow is fully separated along the upper surface of the airfoil with plasma actuator off and vortices appear on the upper surface as well. When the plasma actuator is switched on, the plasma jet makes the separated flow reattached and flow separation disappears, as shown in Figure 2 (b). Therefore, this virtual shape leads to flow separation control.

CONCLUSIONS

The plasma jet by the DBD plasma actuators attached on the leading-edge of a NACA 0012 airfoil has been investigated in still air, where the vorticity, velocity distribution, Reynolds stress and turbulent kinetic energy distribution have been analyzed. This jet would act as a "virtual nose droop" to make the air freestream flow over the airfoil smoothly. Then PIV measurements were conducted with a freestream velocity of 3m/s to study how this jet would affect the flow separation. The results show that the fully separated flow becomes reattached when the plasma actuator is switched on, so this "virtual nose droop" works and controls the flow separation.

REFERENCES

[1] M. P. Patel, Z. H. Sowle, T. C. Corke, and C. He, "Autonomous Sensing and Control of Wing Stall Using a Smart Plasma Slat," J. Aircr., vol. 44, no. 2, pp. 516–527, Mar. 2007.

[2] M. L. Post and T. C. Corke, "Separation Control on HIgh Angle of Attack Airfoil Using Plasma Actuators," AIAA J., vol. 42, no. 11, pp. 2177–2184, Nov. 2004.

[3] M. P. Patel, T. T. Ng, S. Vasudevan, T. C. Corke, and C. He, "Plasma Actuators for Hingeless Aerodynamic Control of an Unmanned Air Vehicle," J. Aircr., vol. 44, no. 4, pp. 1264–1274, Jul. 2007.

[4] A. Vorobiev, R. M. Rennie, E. J. Jumper, and T. E. McLaughlin, "Experimental Investigation of Lift Enhancement and Roll Control Using Plasma Actuators," J. Aircr., vol. 45, no. 4, pp. 1315–1321, Jul. 2008.

[5] R. D. Whalley and K.-S. Choi, "Turbulent boundary-layer control with spanwise travelling waves," J. Phys. Conf. Ser., vol. 318, no. 2, p. 022039, Dec. 2011.

[6] T. N. Jukes and K. Choi, "Turbulent Drag Reduction by Surface Plasma through Spanwise Flow Oscillation," 3rd AIAA Flow Control Conf., no. June, pp. 1–14, 2006.